TRW TAPCO A DIVISION OF
Thompson Ramo Wooldridge Inc.
CLEVELAND 17, OHIO

ER-5084

RESEARCH ON THE VORTEX MHD POWER GENERATOR

SECOND QUARTERLY PROGRESS REPORT

OCTOBER 1962

TAPCO

A Division of

Thompson Ramo Wooldridge Inc.

NASA Contract No. NAS3-2526

TAPCO

A Division of

Thompson Ramo Wooldridge Inc.

SUBJECT: SECOND QUARTERLY PROGRESS REPORT, OCTOBER 1962

CONTRACT NO.: NASA NAS3-2526

TRW PROJECT NO.: 512-009604-08

TITLE: RESEARCH ON THE VORTEX MHD POWER GENERATOR

CONTRIBUTORS:

W. C. Davis
E. L. Krasnoff
W. F. Wade

W. C. Davis
Engineering Specialist

R. T. Craig
Project Manager

I. INTRODUCTION

This report summarizes the efforts during the second quarter of a one-year research program, whose principal objective is the demonstration of feasibility and advancement of the vortex MHD power generator concept. The research is essentially a continuation of the investigation initiated under NASA Contract No. NAS5-703.

Experimental efforts have concentrated on the following: (a) fabrication of an advanced experimental model of a vortex MHD generator; (b) design and fabrication of a gas dilution type of calorimeter for plasma enthalpy measurements; and, (c) fabrication of a vortex chamber for detailed study of the velocity field in a compressible vortex.

Analytical studies have included the application of turbulent boundary layer theory to vortex flow, including the region adjacent to a central body in the vortex.

II. SUMMARY

Fabrication of the experimental model of the vortex MHD generator was completed; this generator is intended to be the primary hardware item in the research program and to serve in the correlation and refinement of existing methods for predicting generator performance.

A review of possible techniques to measure plasma enthalpy was conducted. For purposes of determining local heat transfer coefficients within the vortex generator and also the generator conversion efficiency, a gas dilution type of calorimeter was indicated. A calorimeter was therefore constructed and its initial function will be to determine the enthalpy of the driving jets under conditions similating those within the generator.

Fabrication and installation of the vortex chamber was completed. This is geometrically similar to the vortex generator and is expected to be the major facility which will be employed for a detailed study of the velocity field in a compressible vortex.

The preliminary application of a pseudo-laminar type of turbulent boundary layer analysis to the flow in a vortex containing a porous center body was completed. Further development of this technique now awaits additional experimental data.

Author

III. ITEMS OF PROGRESS

1. Vortex Generator Experiments

Vortex Generator Model. The experimental model of the vortex MHD generator, Figure 1, which was thoroughly described in the previous quarterly report, was fabricated and assembled without any significant difficulty. The components most difficult to fabricate were the water-cooled copper nozzles which required electrical discharge machining. (Subsequent to the period being reported, these nozzles were operated at maximum jet power without any deterioration.) The inner electrode and exhaust tubes, pictured in Figure 2, while initially conceived of as being constructed of a refractory metal, were actually machined from a medium-grain high purity graphite and then sprayed to give a tungsten overlay on the electrode surfaces. The tungsten overlay serves primarily to reduce erosion and corrosion at these critical surfaces. Construction of the inner electrode and exhaust tubes entirely of a refractory metal is feasible but considerably more expensive than the present approach.

Figure 2 illustrates that the generator is capable of being operated with two driving jets; however, the outer electrode pictured is presently prepared for the initial generator operation with a single jet. Not shown in Figure 2 is the internal instrumentation, consisting of thermocouples and pressure port tubing, which will be brought out of the generator through the Conax fittings pictured.

Gas Dilution Calorimeter. Figure 3 shows the gas dilution calorimeter which has been constructed for the purpose of measuring plasma enthalpy, as for example in the efflux of a generator nozzle also pictured here. This type of calorimeter was selected in order to obtain a mean stream enthalpy value and also employs gas dilution as opposed to a water-side heat sink to avoid the possibility of an explosive interaction of a condensed alkali metal and water due to a leak. The operation of the calorimeter is as follows: room temperature nitrogen is supplied to the calorimeter cocurrent with the plasma jet; the three inner tubes shown in the lower part of the picture serve first to direct the unheated nitrogen in a way to protect the calorimeter from direct contact with the high temperature jet and second to thoroughly mix the plasma and nitrogen by two turbulating tantalum screens welded to the center

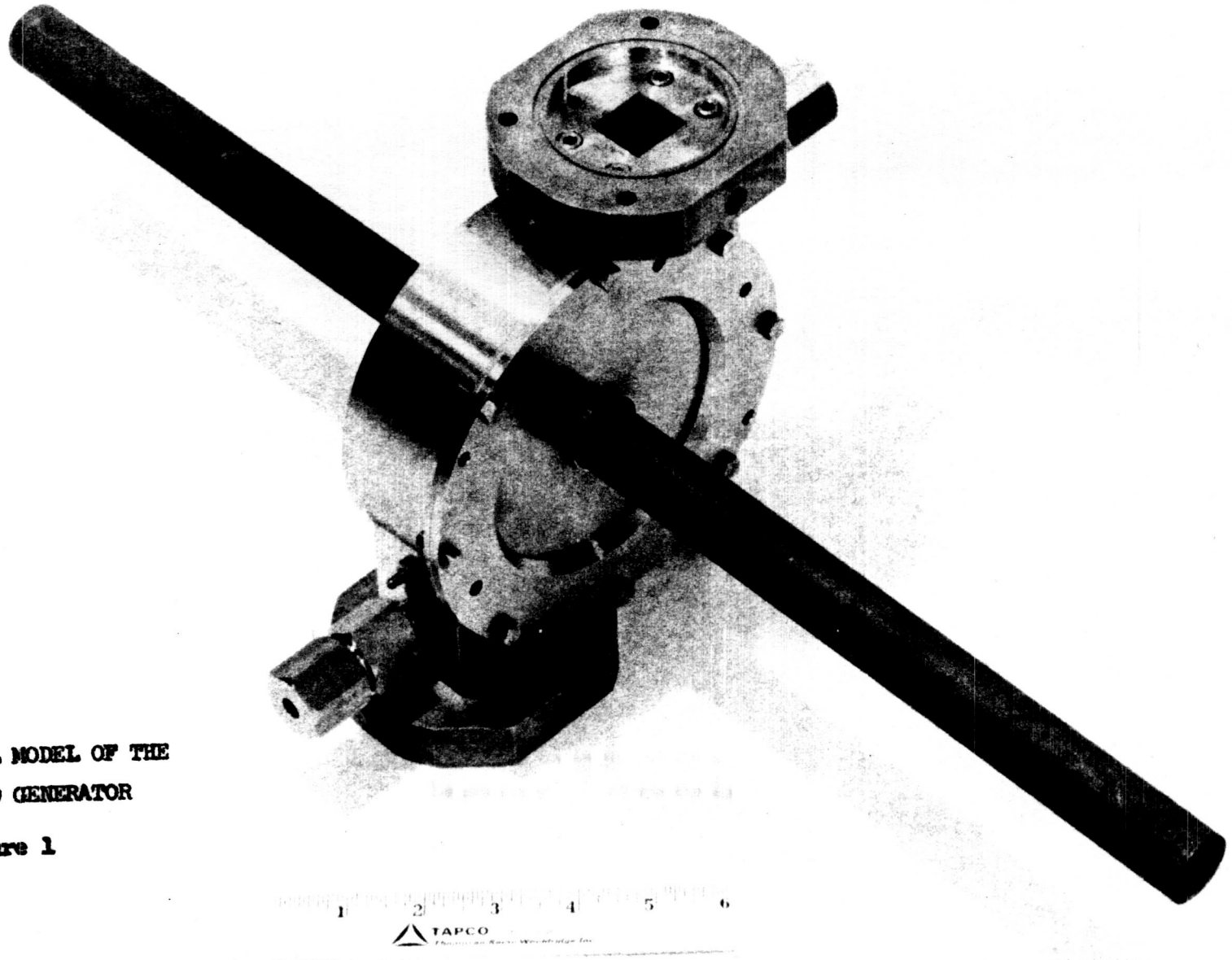

EXPERIMENTAL MODEL OF THE
VORTEX MHD GENERATOR

Figure 1

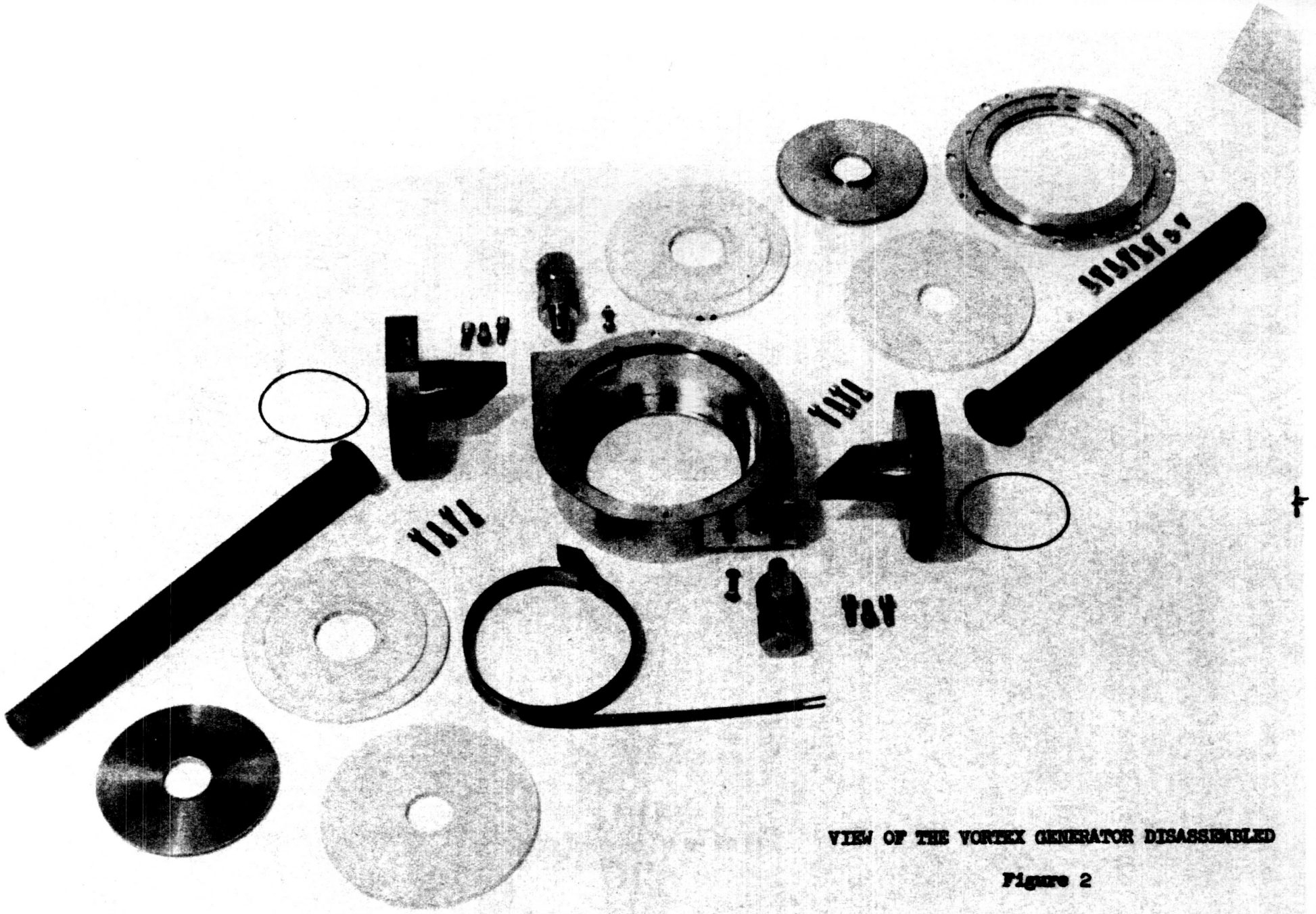

VIEW OF THE VORTEX GENERATOR DISASSEMBLED

Figure 2

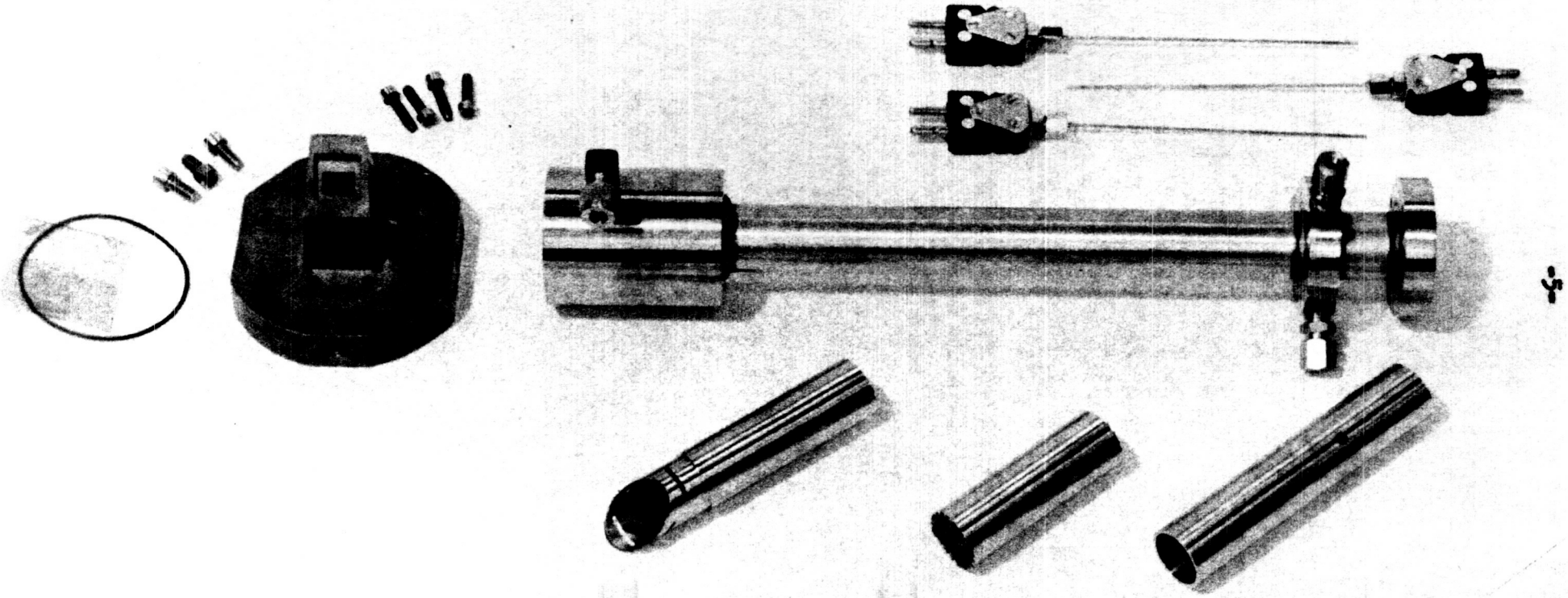

GAS DILUTION CALORIMETER

Figure 3

section; finally an array of thermocouples is employed in determining the average temperatures of the resulting gas mixture diluted to a temperature of approximately 1500°F.

In practice, thermal insulation will be placed around the calorimeter shell to improve accuracy in the calorimetric measurements. Also, an exhaust valve, not shown here, will be secured to the end of the calorimeter and make it possible to vary the back pressure - thus providing means of simulating the generator back pressure which the nozzle will experience in generator tests.

2. Hydrodynamics of the Jet-Driven Vortex

Experimental Program. During this quarter, the basic vortex chamber model was built and prepared for testing. This effort included preparing a set of detail drawings of the chamber components, machining the components, and assembling the model, including the air supply system and the mercury manometer system which will be used to measure static pressures. Figure 4 shows the assembled vortex chamber model, and Figure 5 shows the model, the air supply manifold, and the mercury manometer system.

Analytical Studies. Analytical studies of the hydrodynamics of a jet-driven vortex are now being performed in order to correlate data which is soon to be obtained. The final results of both the experimental and analytical hydrodynamics studies will yield an analytical model which can be employed in vortex chamber optimization studies (with a minimum computational effort.)

Studies of an analytical nature conducted thus far in the present program have been limited to the case of a vortex chamber with a porous wall inner cylinder of the type investigated in Reference 1. In fact, the preliminary analysis of the data of Reference 1 for the case of four driving jets has been completed. As indicated in the first quarterly progress report (Reference 2), the data for the outer region of a vortex chamber (that is, the region adjacent to the outer cylinder and the driving jets) can be correlated by a hydrodynamical model having a constant eddy viscosity and an inner cylinder velocity greater than zero.

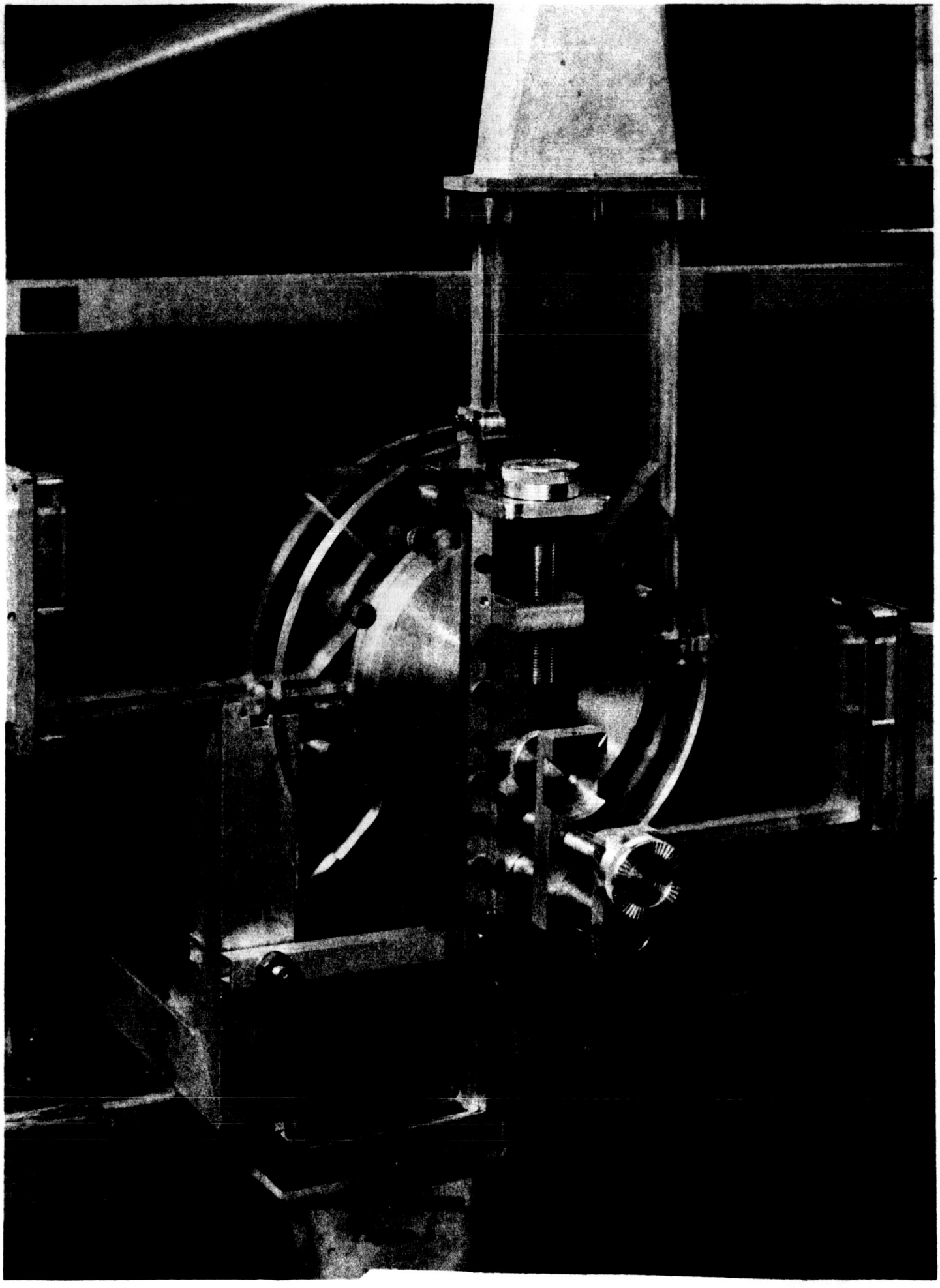

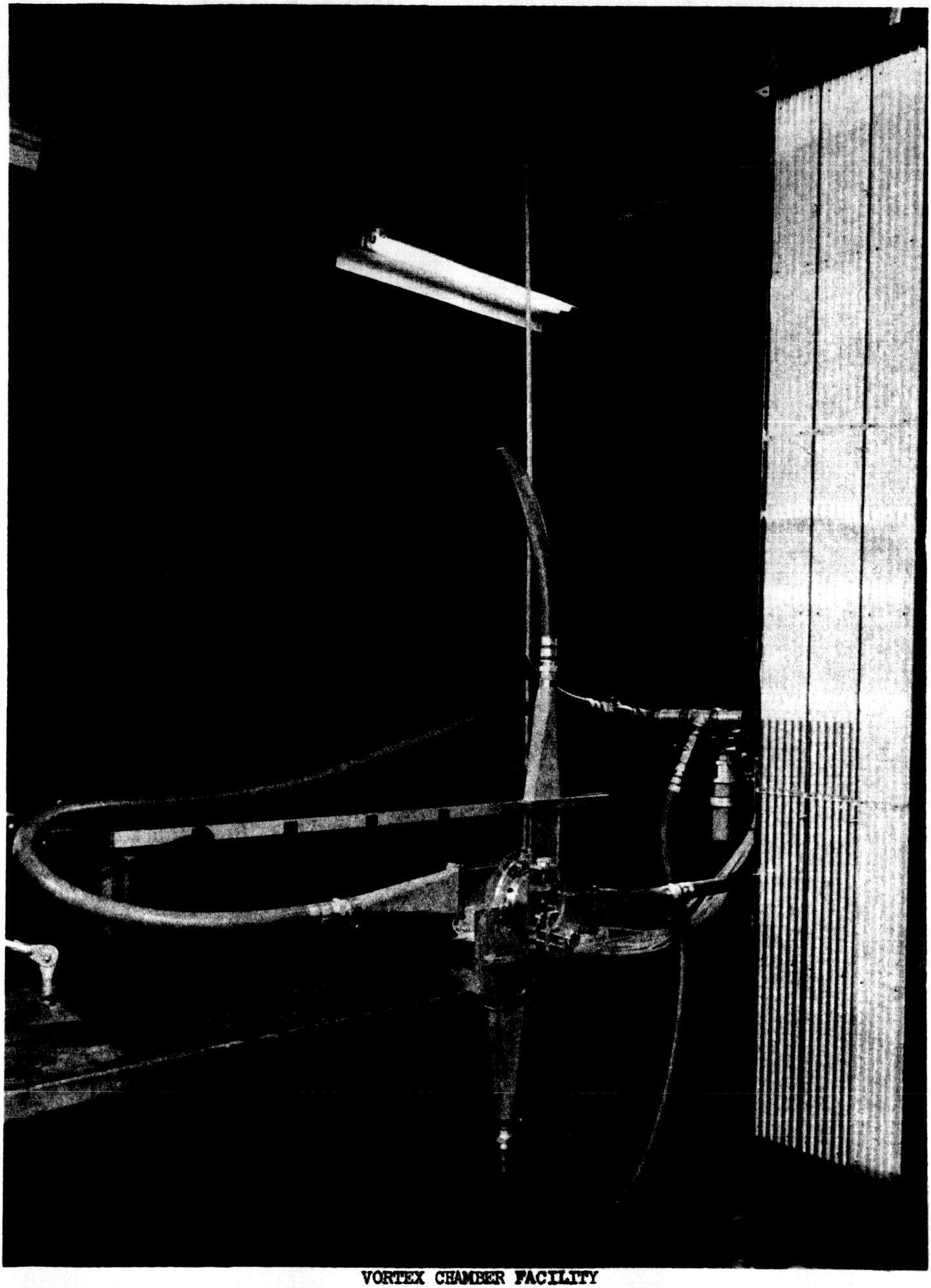

VORTEX CHAMBER FACILITY
Figure 5

The governing differential equation (under the assumption of a constant eddy viscosity which is very much greater than the molecular viscosity) is

$$\frac{N_u}{\left(\frac{\varepsilon_m}{\nu}\right)}\left(\frac{dV}{dR} + \frac{V}{R}\right) = \frac{d}{dR}\left(\frac{dV}{dR} + \frac{V}{R}\right) \tag{1}$$

where v_w = recovered jet velocity

V = v/v_w, dimensionless tangential velocity

r_w = radius at which recovered jet velocity obtains

R = r/r_w, dimensionless radius

Re = $N_u\,(\varepsilon_m/\nu)^{-1}$, effective radial Reynolds number

N_u = $v_w\, r_w/\nu$, radial Reynolds number

ν = viscosity coefficient

ε_m = eddy viscosity in outer region

ν = kinematic viscosity

Employing the boundary conditions $V = V_i$ at $R = R_i$ (where R_i is the dimensionless inner cylinder radius) and $V = 1$ at $R = 1$, the solution of (1) is found to be

$$V = \left[1 - R_i^{-(2 + Re)}\right]^{-1}\left\{\left[1 - V_i R_i^{-(1 + Re)}\right] R^{-1} - (1 - R_i V_i)\, R_i^{-(2 + Re)}\, R^{(1 + Re)}\right\} \tag{2}$$

This expression was fitted to the experimental data of Reference 1 in the region between the outer cylinder and the point of maximum velocity. In so doing, values of Re and V_i were obtained which were then analyzed. In particular, the ratio of eddy to molecular viscosity was found to be given by

$$\left(\frac{\varepsilon_m}{\nu}\right) = \frac{K^2}{2} N_v \tag{3}$$

with (the mixing length constant)

$$K = 0.048 - 1.23\,\frac{u_w}{v_w} \tag{4a}$$

and (the tangential Reynolds number)

$$N_v = \frac{\rho v_w r_w}{\mu} \tag{4b}$$

The form of Equation (3) is suggested by von Karman's similarity hypothesis if use is made of Equation (2) (see e.g., Reference 3). Equation (4) results from a least squares fit of points calculated in the interval $-0.027 \leq (u_w/v_w) \leq 0.0575$. The maximum deviation from this expression was about 15 percent. Values of V_i obtained varied between about 0.95 and 1.15 with an average value of $\overline{V}_i = 1.07$.

The data analyzed thus far has a scatter which does not permit the accurate determination of the ficticious wall velocity, V_i. On the other hand, the value of V_i is of little interest since the outer profile as determined above merges with an inner profile whose velocity vanishes at the inner porous cylinder. In the present case, the inner region near the porous wall is determined as described below. In the case of a vortex chamber having no inner cylinder, V_i is never introduced and the outer region profile is matched to an inner solution in the manner of Reference 4.

The vortex profile in the outer region determines the inner wall friction by conservation of angular momentum. In the dimensionless variables, conservation of angular momentum applied between the inner cylinder and some larger radius is stated by

$$R_i^2 C_{f_i} = R^2 C_f - 2(u_w/v_w) RV \tag{5}$$

where C_f is the friction coefficient

$$C_f = \frac{\tau}{\frac{1}{2}\rho v_w^2} = \frac{2(\varepsilon_m/\nu)}{N_v}\left(\frac{dV}{dR} - \frac{V}{R}\right) \tag{6}$$

Making use of (3) now, there results

$$C_f = K^2\left(\frac{dV}{dR} - \frac{V}{R}\right) \tag{7}$$

and this was used together with (2), (4) and (5) to calculate the inner cylinder friction coefficient. The result, again based on a least squares fit in the interval $0.027 \leq (u_w/v_w) \leq 0.0575$, is

$$C_f = -4.94\,(u_w/v_w) \tag{8}$$

Once the outer region has been determined and C_{f_i} and ε_m are known, attention can be concentrated on the wall regions (near the inner cylinder). Consider first the region immediately adjacent to the inner cylinder. In this laminar sublayer the eddy viscosity is small compared to the molecular viscosity and the basic differential equation for the tangential velocity is

$$N_u\left(\frac{dV}{dR} + \frac{V}{R}\right) = \frac{d}{dR}\left(\frac{dV}{dR} + \frac{V}{R}\right) \tag{9}$$

Solving this with the boundary conditions $V = 0$ at $R = R_i$ and

$$\frac{dV}{dR} = \frac{N_v\, C_{f_i}}{2}$$

at $R = R_i$ there is obtained

$$V_s = \frac{N_v\, C_{f_i}}{2(2 + N_u)}\left\{\frac{R}{R_i}^{\frac{1 + N_u}{N_u}} - \frac{R_i^2}{R}\right\} \tag{10}$$

where the subscript s denotes that the expression holds only in the laminar sublayer.

Now the region adjacent to the outer region can be referred to as the wall region in analogy to the universal wall law region of ordinary turbulent boundary layer theory. In this wall region, the eddy viscosity is large compared to the molecular viscosity but it varies with distance from the inner cylinder. In this case, the basic equation is again (1) with Re depending on R. Displaying N_u and $\varepsilon/\mu = \varepsilon(R)/\mu$ it is

$$\frac{N_u}{\varepsilon(R)/\mu}\left(\frac{dV}{dR} + \frac{V}{R}\right) = \frac{d}{dR}\left(\frac{dV}{dR} - \frac{V}{R}\right) \tag{11}$$

This equation can be integrated and the desired result, $V = V(R)$, given in closed form for a variety of assumed variations of $\varepsilon/\mu = \varepsilon(R)/\mu$. Unfortunately no data exists as yet on which to base a choice. To illustrate the procedure, however, consider a linear variation of ε/μ from zero at the inner cylinder to (ε_m/μ) at the matching point (which is to be determined by noting where experimental data began to depart from the outer profile of Equation (2). In this case

$$\varepsilon(R)/\mu = a + b\,R$$

and the solution to (11) is

$$V = \frac{CI(R) + B}{R} \tag{12}$$

where

$$I(R) = \int^{R} \frac{R^{1 + \frac{N_u}{a}}\, dR}{(a + b\,R)^{\frac{N_u}{a}}} \approx \frac{R^{1 + \frac{N_u}{a}}\, (\varepsilon/\mu)}{b\,(1 - \frac{N_u}{a})} \tag{13}$$

The expression on the extreme right of (13) was obtained by holding the numerator constant during the integration. This can be done with little loss of accuracy since the numerator is very slowly varying compared with the denominator.

The constants B and C may be determined by matching V and its first derivative to the profile of the outer region (at the assumed matching point).

The "transition" region between the sublayer and the wall region is defined by $\varepsilon/\mu = 0$ (1). Here the relevant differential equation is again (11) if ε/μ is replaced by $1 + \varepsilon/\mu$. Then, if $1 + \varepsilon/\mu = a' + b'\,R$ in the transition region, the solution is again (12) and (13) if ε/μ is replaced by $1 + \varepsilon/\mu$ in the latter. The constants B and C in this case are to be determined by again matching V and its first derivative to the wall region profile.

The results of the procedure outlined above as applied to an example with $u_w/v_w = -0.0575$ and $N_u = -3100$ are shown in Figure 6. The abscissa is the normalized radius

$$\bar{R} = \frac{R - R_i}{1 - R_i} = \frac{r - r_i}{r_w - r_i}$$

and ε/μ was assumed to decrease linearly from its maximum value at $\bar{R} = 0.1$ to 20 at $\bar{R} = 0.01$ and then linearly to zero at $\bar{R} = 0$.

The mismatch between the laminar sublayer and the transition region indicated in Figure 6 is caused primarily by the assumed ε/μ variation and by the

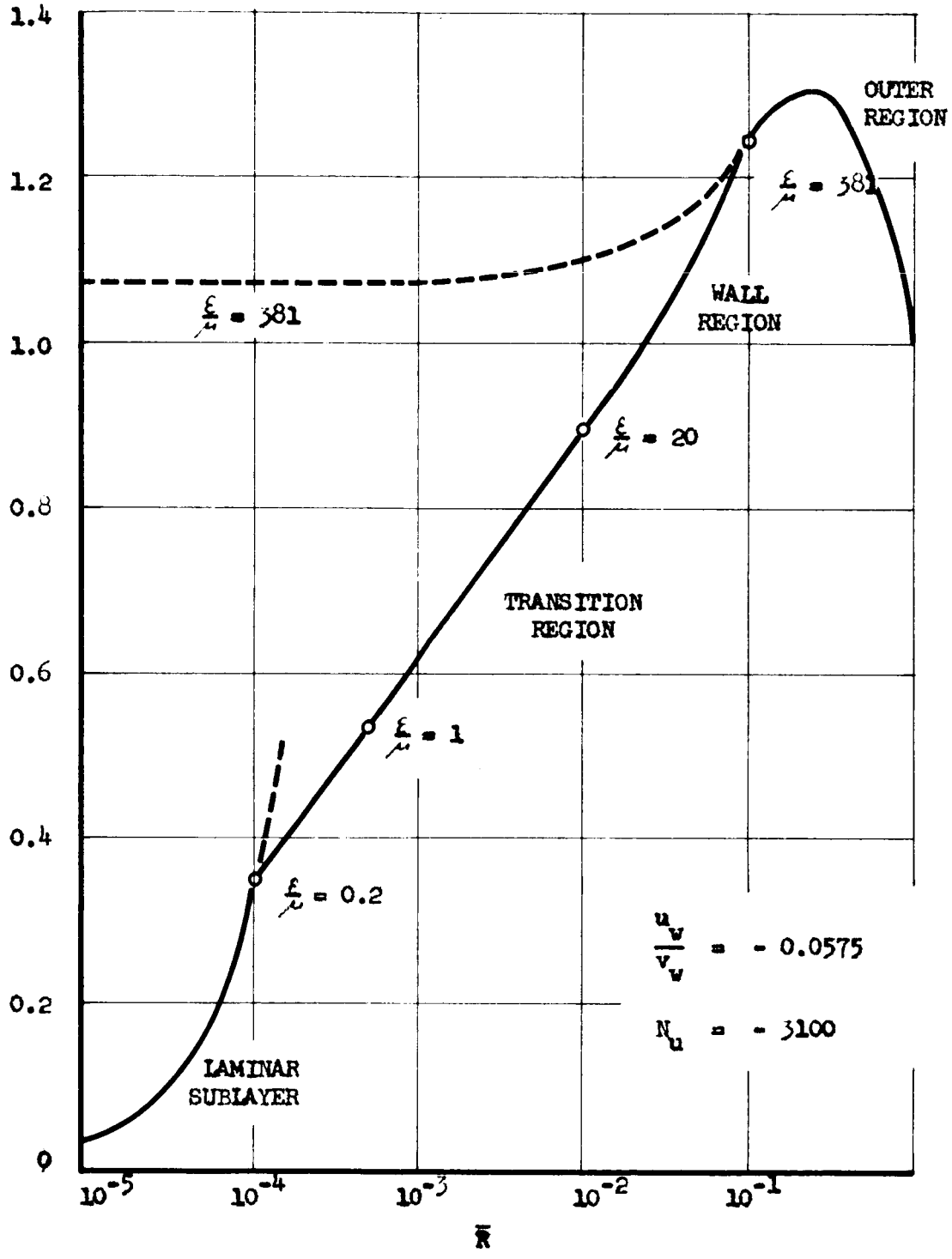

THE INNER WALL REGIONS
OF THE VORTEX CHAMBER

Figure 6

accuracy of the data which defines the inner wall friction coefficient and therefore the sublayer profile [see (10)].

It should be noted that data of Reference 1 for the wall region consists of only one point for each pair $\left[(u_w/v_w),\ N_u\right]$ of independent variables. This point is at $\bar{R} = 0.075$ which corresponds to a distance of less than one-tenth of an inch from the inner cylinder. Thus, since the experimental profiles of Reference 1 were obtained from wall static pressure measurements, the accuracy of the result at $\bar{R} = 0.075$ is questionable (compared to the points in the outer region). The reason for this suggestion is related to secondary flow effects in the corners formed by the inner cylinder and the side-walls of the vortex chamber.

In any event insufficient data exist to test Equation (11) with any assumed function $\xi(R)/\mu$. This must be deferred until the velocity probe data of the current research program have been obtained.

IV. INTERPRETATION OF RESULTS AND CONCLUSION

Fabrication of the vortex MHD generator experimental model was completed and appears to be satisfactory in its conceptual design. Initial operation of the generator will be underway soon, following minor modifications to the magnet structure which will accommodate air coolant passages for generator temperature control. After accomplishing the check out of generator operation, the test program will be underway and have as its principal objective the evaluation of generator performance prediction methods.

The vortex chamber installation was completed and soon will be providing more comprehensive and accurate data for the determination of velocity fields within vortex cavities supplied with and without center bodies.

Further study of the application of pseudo-laminar boundary layer analysis to the prediction of velocity profiles within a turbulent vortex confirmed the earlier expectations of its successful employment. This phase of study is essentially complete but will be reviewed as soon as more accurate data are obtained from the vortex chamber experiments, especially in the region of the center bodies.

V. REFERENCES

1. G. G. Williamson and J. E. McCune, "A Preliminary Study of the Structure of Turbulent Vortices", ARAP Report No. 32, July 1961.

2. W. C. Davis et al, "Research on the Vortex MHD Power Generator, First Quarterly Progress Report", TRW ER-4949, July 1962.

3. R. C. Ragsdale, "Applicability of Mixing Length Theory to a Turbulent Vortex System", NASA TN D-1051, August 1961.

4. M. L. Rosenzweig, "Velocity Recovery and Shear Reduction in Jet Driven Vortex Tubes", Aerospace Corp., Report No. TDR-594 (1203-01)TN-1, March 1961.

DISTRIBUTION LIST FOR QUARTERLY AND FINAL REPORTS FOR

CONTRACT NAS3-2526

National Aeronautics and Space Administration
1512 H. Street, N.W.
Washington 25, D. C.
Attention: Walter Scott (RP) — 2 copies

National Aeronautics and Space Administration
1512 H. Street, N.W.
Washington 25, D. C.
Attention: Herbert Rochen (RNEP)

Ames Research Center
National Aeronautics and Space Administration
Moffett Field, California
Attention: Librarian

Goddard Space Flight Center
National Aeronautics and Space Administration
Greenbelt, Maryland
Attention: Librarian

Langley Research Center
National Aeronautics and Space Administration
Hampton, Virginia
Attention: Librarian

Lewis Research Center
National Aeronautics and Space Administration
21000 Brookpark Road
Cleveland 35, Ohio
Attention: Librarian — 2 copies

Jet Propulsion Laboratory
National Aeronautics and Space Administration
Pasadena, California
Attention: Librarian

Marshall Space Flight Center
National Aeronautics and Space Administration
Huntsville, Alabama
Attention: Librarian

Manned Spacecraft Center
National Aeronautics and Space Administration
Houston, Texas
Attention: Librarian

Lewis Research Center
National Aeronautics and Space Administration
21000 Brookpark Road
Cleveland 35, Ohio
Attention: Henry O. Slone - SEPO

Lewis Research Center
National Aeronautics and Space Administration
21000 Brookpark Road
Cleveland 35, Ohio
Attention: John J. Fackler - SEPPO

Lewis Research Center
National Aeronautics and Space Administration
21000 Brookpark Road
Cleveland 35, Ohio
Attention: Bernard Lubarsky - SPD

Lewis Research Center
National Aeronautics and Space Administration
21000 Brookpark Road
Cleveland 35, Ohio
Attention: Norman T. Musial - Patent Counsel

Lewis Research Center
National Aeronautics and Space Administration
21000 Brookpark Road
Cleveland 35, Ohio
Attention: Richard Geye - SEPO

Lewis Research Center
National Aeronautics and Space Administration
21000 Brookpark Road
Cleveland 35, Ohio
Attention: John Heighway - APD

Lewis Research Center
National Aeronautics and Space Administration
21000 Brookpark Road
Cleveland 35, Ohio
Attention: Herman Schwartz - SEPO — 2 copies (and a reproducible copy)

Advanced Research Project Agency
Pentagon, Washington 25, D. C.
Attention: John Huth

Aeronautical Systems Division
Flight Accessories Laboratory
Wright-Patterson Air Force Base, Ohio
Attention: Donald Warnock

U. S. Air Force
Office of Scientific Research
Washington 25, D. C.
Attention: M. M. Slawsky

MHD Research
Newport Beach,
California
Attention: Donald Howard

U. S. Army Signal Research Development Laboratory
Fort Monmouth, New Jersey
Attention: Arthur Daniel

U. S. Atomic Energy Commission
Technical Reports Library
Washington 25, D. C.
Attention: J. M. O'Leary — 3 copies

U. S. Atomic Energy Commission
Technical Information Service Extension
P. O. Box 62
Oak Ridge, Tennessee — 3 copies

Institute for Defense Analysis
1825 Connecticut Avenue, N.W.
Washington 9, D. C.
Attention: Robert Hamilton

The Rand Corporation
1700 Main Street
Santa Monica, California
Attention: Librarian

Airesearch Manufacturing Division
The Garrett Corporation
Phoenix, Arizona
Attention: Librarian

Allison Division
General Motors Corporation
Indianapolis 6, Indiana
Attention: Librarian

Electro-Optical Systems Inc.
125 N. Vinedo Avenue
Pasadena, California
Attention: Joseph Neustein

General Electric Company
Missile and Space Vehicle Division
Valley Forge, Pennsylvania
Attention: George W. Sutton

Pratt and Whitney Aircraft
400 Main Street
East Hartford 8, Connecticut
Attention: William Podolny

Atomics International
8900 DeSoto Avenue
Canoga Park, California
Attention: Librarian

Avco, R and D Division
201 Lowell Street
Wilmington, Massachusetts
Attention: Librarian

Plasmadyne Corporation
4839 South Main Street
Santa Ana, California
Attention: Librarian

Westinghouse Electric Corporation
Research Laboratories
Churchill Burrough
Pittsburgh, Pennsylvania
Attention: Librarian

Westinghouse Electric Corporation
Astronuclear Laboratory
250 Mt. Lebanon Blvd.
Pittsburgh 34, Pennsylvania
Attention: Librarian

The Martin Company
Nuclear Division
P. O. Box 5042
Baltimore 20, Maryland
Attention: Librarian

Materials Research Corporation
Orangeburgh, New York
Attention: Vernon E. Adler

Commanding Officer
U. S. Naval Underwater Ordnance Station
Newport, Rhode Island
Reference: Ad3(WSD)wsd 5600/1